Anisotropic effective mass of orthoexcitons in Cu_2O

Dietmar Fröhlich,* Jan Brandt, Christian Sandfort, and Manfred Bayer
Fakultät Physik, Technische Universität Dortmund, DE-44221 Dortmund, Germany

Heinrich Stolz
Fachbereich Physik, Universität Rostock, DE-18051 Rostock, Germany

(Received 22 June 2011; revised manuscript received 25 August 2011; published 28 November 2011)

Most of the parameters of the lowest excitons of Cu_2O (1S excitons of yellow series) are very well known by now. After the experimental determination of the 1S paraexciton mass by two-phonon spectroscopy, a reliable parameter for the determination of orthoexciton masses is now available. Anisotropic mass values are expected for the threefold 1S orthoexciton, because of isotropic and anisotropic k^2 exchange terms. Taking into account the paraexciton mass ($2.61\,m_0$) instead of the previously used sum of bare band masses ($1.64\,m_0$), earlier orthoexciton mass values have to be revised. Again by two-phonon spectroscopy now of orthoexcitons the only unknown parameter Δ_1 (isotropic k^2 exchange) is determined experimentally, which then allows a reliable determination of orthoexciton mass values in **k** space.

DOI: 10.1103/PhysRevB.84.193205 PACS number(s): 78.20.−e, 71.35.Cc, 71.36.+c

I. INTRODUCTION

The yellow exciton series in Cu_2O has become a textbook example after the first observation about 60 years ago.[1] In the beginning, there were mainly the Leningrad[2] and the Strasbourg group[3] who studied many details in the rich spectra of the lowest exciton series. It is termed the yellow series though it starts in the red (about 610 nm) but reaches out into the yellow (570 nm) with a perfect hydrogenlike P series from $n = 2$ to $n = 12$.[4] In a next experimental step forward, two-photon absorption spectroscopy was applied which revealed a fine structure of even-parity excitons (S and D excitons) up to $n = 5$.[5] By two-photon excitation spectroscopy S-D excitons were resolved up to $n = 7$.[4] Up to then the 1S exciton was assumed to consist of a triply degenarate orthoexciton state and a single paraexciton as expected from symmetry considerations.[6] Recently it was shown by high-resolution spectroscopy that this degeneracy is lifted by wave-vector-dependent exchange interaction.[7] It was soon recognized that the k^2 dependence leads to anisotropic effective mass values.[8,9] From the **k**-dependent splitting three parameters (Δ_3, Δ_5, and Δ_Q) were determined. A fourth parameter Δ_1 (isotropic k^2 term) is expected from symmetry analysis but it does not lead to a splitting and therefore cannot be directly determined since it does not lead to a spectroscopic signature.

In order to calculate effective masses, all these parameters are of relevance and, in addition, the mass value without exchange interaction, which is the paraexciton mass. In the analysis of Refs. 7 and 8 the sum of the band masses ($1.64\,m_0$) (Ref. 10) was taken for the paraexciton mass and for the average of the orthoexciton mass $m = 3.0\,m_0$ from the literature.[11] In the previous analysis of Refs. 7 and 8 we derived from the above assumptions for the isotropic k^2-dependent exchange parameter $\Delta_1 = -8.6\ \mu$eV, which led, e.g., for the quadrupole forbidden orthoexciton component ΔE_2 in $\mathbf{k} \parallel [001]$ to a mass $M_2 = 5.4$. Recently, the paraexciton mass $M_P = 2.61$ (in units of the free electron mass m_0) was determined by two-phonon excitation spectroscopy,[12] which will now be used instead of the sum of the band masses.

As in the case of the paraexciton,[12] we apply a kinematical analysis of two-phonon excitation spectroscopy for the orthoexciton with laser wave vectors along a [110] crystalline direction. From these experiments the exchange parameter Δ_1 can be determined and thus with the known parameters Δ_3, Δ_5, and Δ_Q the mass values for all orthoexciton components and all **k** directions can be derived.

The paper is organized as follows. In Sec. II the outline of the method of two-phonon excitation spectroscopy and its analysis for the three nondegenerate orthoexcitons for $\mathbf{k} \parallel [110]$ are presented. After a short description of the experimental setup in Sec. III, in Sec. IV the experimental results and the revised orthoexciton mass values are discussed, followed by our conclusions.

II. THEORY

The Rydberg deduced from the yellow nP-exciton series is 98 meV,[4] but the binding energy of the 1S paraexciton is $E_b = 151.6$ meV as derived from the band gap energy ($E_g = 2.172\,20$ eV)[4] and the paraexciton resonance ($E_P = 2.020\,598$ eV).[12] With an exchange splitting of 12.1 meV (Ref. 13) the orthoexciton binding energy is $E_b = 139.5$ meV. The deviation of the 1S-exciton binding energy from the hydrogenlike series originates from the small 1S-exciton Bohr radius of 0.8 nm (Ref. 14) together with the strong nonparabolicity of the Γ_7^+ valence band,[15] which leads to strong central-cell corrections for both the binding energy and the exciton effective mass. In a previous analysis, Ref. 16, it was deduced that the masses of the ortho- and paraexciton 1S states are the same $m = 3\,m_0$, while the higher exction states have the sum of the bare band masses $1.68\,m_0$. By high-resolution laser spectroscopy, however, it was shown that there is an anisotropic k^2-dependent exchange interaction resulting in an anisotropic orthoexciton mass.[8,9] The analysis revealed the exchange parameters Δ_1, Δ_3, Δ_5, and Δ_Q. In this analysis, however, it was assumed that the deviation of the orthoexciton mass from the sum of the band masses is solely due to the k^2-exchange terms. Since there are no k^2-exchange terms for the paraexciton this yields a too

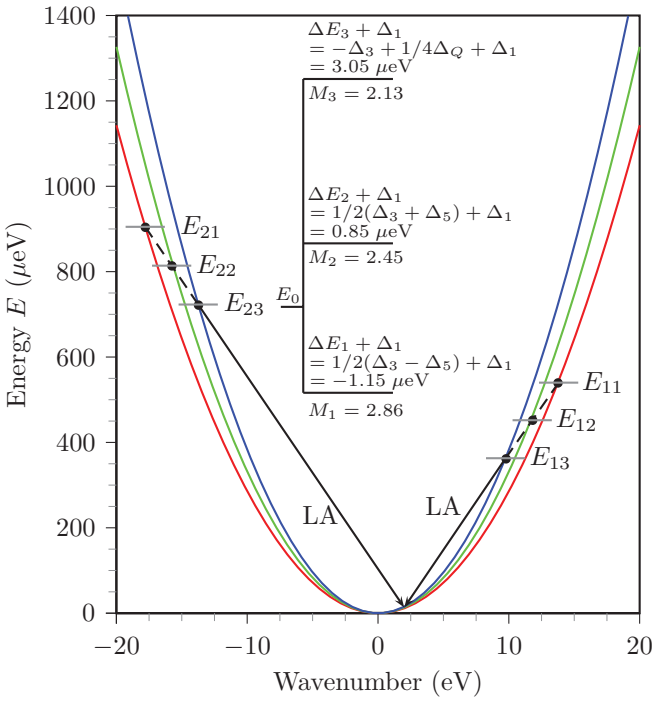

FIG. 1. (Color online) Schematics of longitudinal acoustic (LA)-phonon scattering in the three orthoexciton parabolas for $\mathbf{k} \parallel [110]$. Crossings of the LA-phonon line with the parabolas mark the range of resonant two-phonon scattering. Inset: Splitting of the three orthoexciton states at $k = k_0$ and masses of the three states taking $\Delta_1 = 0.5\ \mu$eV from the analysis in Sec. IV.

low mass of $1.64\,m_0$, contrary to the central-cell corrections needed to explain the large binding energy.[16] By two-phonon excitation spectroscopy and a merely kinematical analysis the paraexciton mass was determined to be $2.61\,m_0$.[12] This mass value can now be used to derive orthoexciton band masses solely from the k^2-exchange terms. As in Ref. 12 we assume that any hole anisotropy and central-cell corrections are included in the paraexciton mass and therefore already taken into account in the determination of the orthoexciton mass since one deals with the same orbital content as in the paraexciton.

The exchange parameters Δ_3, Δ_5, and Δ_Q are well known[7] but symmetry considerations allow a fourth parameter, Δ_1, which is due to a possible isotropic k^2 contribution. Thus Δ_1 cannot be derived by mere absorption measurements for different $\mathbf{k}$ directions. In Refs. 7 and 8 this parameter was calculated to be $-8.6\ \mu$eV by assuming the wrong paraexciton mass of $1.64\,m_0$ (Ref. 10) and an orthoexciton mass of $3\,m_0$.[11] In a more recent publication there was a mass value of $2.7\,m_0$ reported.[17] In order to determine Δ_1 experimentally, we again apply two-phonon excitation spectroscopy.

As sketched in the inset of Fig. 1, for a sample oriented along [110] the degeneracy is fully lifted.[7] Contrary to the paraexciton analysis, there are now three different mass values, M_i, expected. The corresponding three orthoexciton parabolas are shown. Due to its flat dispersion, the optical phonon (energy E_{LO}) can contribute with any $\mathbf{k}$ and excite any of the three orthoexciton components E_{0i} in $\mathbf{k}$ space. This gives rise to the well-known anti-Stokes phonon sideband[11] with the onset at $E_0 + E_{\mathrm{LO}}$ (ingoing resonance). This resonance is monitored by the quadrupole emission of the allowed component ($E_{02} = E_0 + \Delta E_2 + \Delta_1$, Fig. 1) which is shifted by $E_{\mathrm{LO}} = 10.58$ meV (Ref. 12) to lower energy (outgoing resonance). Tuning the laser to higher energies $E_L > E_0 + E_{\mathrm{LO}}$, further resonances due to forward and backward scattering of acoustic phonons are expected as was demonstrated for the paraexciton.[12] As indicated in Fig. 1 we now expect six resonances, E_{1i} and E_{2i} ($i = 1,2,3$). As mentioned before, the only unknown parameter is the isotropic k^2 term Δ_1.

As an example we discuss the anisotropic masses for $\mathbf{k} \parallel [110]$, since in this wave-vector direction the degeneracy is fully lifted (inset of Fig. 1). We thus expect three mass values, $M(\Delta E_i, \Delta_1)$. They can be calculated from the paraexciton mass M_P, ΔE_i, and Δ_1:

$$\frac{\hbar^2 k_0^2}{2M_P\, m_0} + \Delta E_i + \Delta_1 = \frac{\hbar^2 k_0^2}{2M_i\, m_0}, \tag{1}$$

where k_0 is the wave number at resonance and m_0 the free electron mass. For convenience we introduce $x = \hbar c k/n$ (eV) instead of the wave number k (m^{-1}) (Ref. 18) where n is the refractive index ($n = 2.94$)[12] and $x_0 = E_0 = 2.032\,78$ eV is the resonance energy at k_0. The ΔE_i values are calculated from the known anisotropy parameters[7] ($\Delta_3 = -1.3\ \mu$eV, $\Delta_5 = 2\ \mu$eV, and $\Delta_Q = 5\ \mu$eV) as shown in the inset of Fig. 1. As mentioned in the Introduction, the same value of an isotropic contribution (Δ_1) has to be added to each ΔE_i, which will be determined by two-phonon excitation spectroscopy. From Eq. (1) we get

$$M_i = [1 + (\Delta E_i + \Delta_1) C M_P]^{-1} M_P, \tag{2}$$

where

$$C = \frac{2m_0c^2}{E_0^2 n^2} = 2.8614 \times 10^4\ \mathrm{eV}^{-1} \tag{3}$$

with the vacuum velocity of light c. The three exciton parabolas $E_i(x)$ in Fig. 1 are calculated from the mass values, M_i:

$$E_i(x) = \frac{x^2 n^2}{2M_i m_0 c^2}. \tag{4}$$

For the determination of the mass values, M_i, we used in addition to the known anisotropy energy shifts, ΔE_i, for the isotropic exchange parameter $\Delta_1 = 0.5\ \mu$eV, which is gained from our experimental results as outlined in Sec. IV. For forward and backward scattering by longitudinal acoustic phonons (LA phonons) we now expect six resonances (E_{1i} and E_{2i}, $i = 1,2,3$) instead of two as in the case of the paraexciton.[12] E_{1i} and E_{2i} refer to the forward and backward resonances, respectively. Note that these energy values are shifts with respect to the corresponding resonances, E_{0i}. From a simple kinematical analysis,[12] we derive the following for these shifts:

$$\begin{aligned} E_{1i} &= \left(\frac{v}{c}\right)^2 2M_i m_0 c^2 - \left(\frac{v}{c}\right) 2E_{0i} n, \\ E_{2i} &= \left(\frac{v}{c}\right)^2 2M_i m_0 c^2 + \left(\frac{v}{c}\right) 2E_{0i} n, \end{aligned} \tag{5}$$

where $v = 4.63 \times 10^3\ \mathrm{ms}^{-1}$ is the sound velocity for LA phonons.[12]

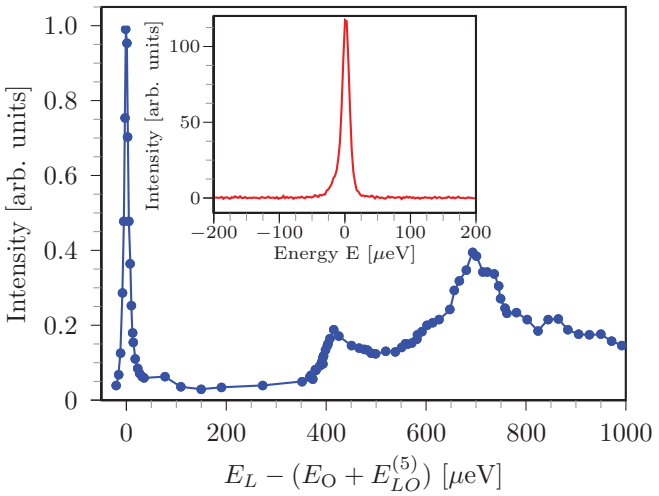

FIG. 2. (Color online) Two-phonon excitation spectrum of orthoexcitons for $\mathbf{k} \parallel [110]$; inset, quadrupole emission of ΔE_2 component, spectral width limited by monochromator (7 μeV), $E = 0$ corresponds to 2.032 78 eV.

From the onset of forward LA scattering ($E_{1,2}$, Fig. 1), we determine Δ_1, which is then used together with the known parameters, ΔE_i, to calculate the mass values, M_i [Eq. (2)]. We insert Eq. (2) in the first of Eq. (5) and solve it for Δ_1:

$$\Delta_1 = \frac{\left(\frac{v}{c}\right)^2 E_0^2 n^2}{E_{1,2} + 2\frac{v}{c}E_0 n} - (CM_P)^{-1} - \Delta E_2. \qquad (6)$$

In this simple analysis only scattering processes in the energy-k plane of the exciting laser are considered. Though the $\mathbf{k}$ vector of excitation is fixed to [110], the subsequent two-phonon processes (LA and optical phonon) allow energy- and momentum-conserving processes in full $\mathbf{k}$ space ending in the quadrupole emission again with $\mathbf{k} \parallel [110]$. In the case of the single paraexciton, the simple analysis,[12] considering only processes in the energy-k plane of the exciting laser, led to accurate E_1 and E_2 values from which the paraexciton mass $M_P = 2.61$ was derived. Because of the threefold orthoexciton as compared to the single paraexciton, we expect a more complicated two-phonon excitation spectrum, the analysis of which has to take into account relaxation processes between the three orthoexciton components. If we assume, however, that the onset of the spectrum is dominated by the emission from the quadrupole allowed component ΔE_2 (inset Fig. 1), we get a fit for the only unknown parameter, Δ_1.

III. EXPERIMENT

The experimental setup of high-resolution spectroscopy is described in detail in previous publications.[7,12] Contrary to the determination of the paraexciton mass,[12] there is no magnetic field necessary, since orthoexcitons are allowed for quadrupole transitions. For the two-phonon excitation spectroscopy we used the quadrupole emission of the orthoexciton (outgoing resonance) to monitor the two-phonon (Γ_5^- optical and longitudinal acoustic phonon, ingoing resonance) excitation process as a function of laser energy. The laser energy (bandwidth of laser about 5 neV) was monitored by a wave meter with an accuracy of 100 neV. The wave meter determines the resolution of the excitation spectrum, whereas the accuracy of energy readings in the spectrum and the final results are limited by the width of the phonon line of 10 μeV. For the measurements the same sample as in Ref. 12 [thickness of 250 μm, oriented along (110)] was used. As mentioned before, strain-free mounting of the sample is of great importance since otherwise the linewidth of the orthoexciton quadrupole resonance increases above the 10 μeV of the phonon line. Additionally, a narrower quadrupole emission line improves discrimination of the signal against the noise background. The measurements were done at a temperature of about 1.3 K.

IV. RESULTS AND DISCUSSION

We now present our experimental results. As the k^2-dependent exchange interaction lifts the degeneracy and leads to different anisotropic masses of the orthoexciton states, the spectrum is expected to be far more rich and complicated as compared to the paraexciton case.[12] In Fig. 2 the two-phonon excitation spectrum is shown, which is obtained by tuning the laser one $^3\Gamma_5^-$ optical phonon above the orthoexciton resonance to higher energies. The sharp peak at $E = 0$ corresponds to the Raman transition of the $^3\Gamma_5^-$ phonon to the state at k_0. Since we observe the emission in the [110] direction

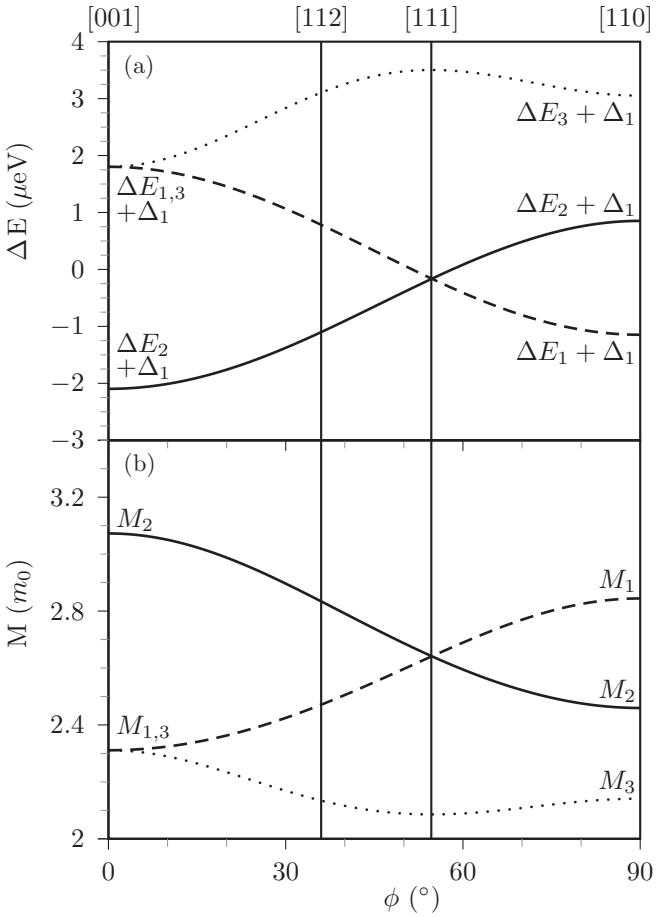

FIG. 3. (a) Exchange shifts of orthoexcitons as a function of ϕ; $\mathbf{k}$ lies in the [001]–[110] plane. (b) Effective exciton mass as a function of ϕ.

(inset Fig. 2), we monitor the quadrupole allowed component $\Delta E_2 + \Delta_1$ (Fig. 1). We assume that the onset of the forward LA scattering is dominated by the quadrupole allowed E_{12} process. From the onset of the spectrum in Fig. 2 we derive $E_{12} = (410 \pm 10)\ \mu$eV. Inserting this value into Eq. (6) yields $\Delta_1 = (0.5 \pm 0.3)\ \mu$eV.

From these values we can derive orthoexciton mass values within an error bar of ± 0.2. In Fig. (3) we present the **k** dependence of the energy splitting $\Delta E(k_0)$ and the mass value $M(\mathbf{k})$ for selected directions in **k** space. This plot has to be compared with our previous results (Fig. 10 in Ref. 8, Fig. 1 in Ref. 9). For example, for $\mathbf{k} \parallel [001]$ we now obtain $M_2([001]) = 3.1 \pm 0.2$ in contrast to $M_2([001)] = 5.4$ in the previous results. It has to be noted that the error bar of the orthoexciton masses (± 0.2) is larger than that of the paraexciton mass (± 0.04).

In two former experiments an orthoexciton mass of $M = 3$ was derived.[11,19] In both experiments the orientation of the studied sample was not reported. In addition the limited spectral resolution made it impossible to determine any mass anisotropy. Therefore a comparison with our **k**-dependent mass values in Fig. 3 is not possible.

V. CONCLUSIONS

In this contribution we present anisotropic mass values of the orthoexcitons in Cu_2O, which are based on the paraexction mass of $2.61\, m_0$ and an experimental value for the isotropic **k**-dependent exchange constant $\Delta_1 = 0.5 \pm 0.3$, which was gained by two-phonon spectroscopy. With this value and the exchange parameter ΔE_i we calculate for selected directions in **k** space for all three components the orthoexciton mass $M_i(\mathbf{k})$. For $M_2([001])$ we now get 3.1 ± 0.2, which is much more reasonable than the previous value of 5.4.[8,9]

For more recent discussions of ortho- and paraexciton mass values we refer to Refs. 20 and 21. In Ref. 20 interesting consequences of anisotropic mass values of the orthoexciton are discussed. They are based, however, on wrong mass values presented in Refs. 8 and 9. As mentioned before, it is the main aim of this contribution to correct these mass values. As shown in Fig. 3 there is still a considerable spread of mass values for different **k** directions. For $\mathbf{k} \parallel [111]$ we get the minimum mass $M = 2.1$, whereas a maximum mass value of $M = 3.1$ is found for $\mathbf{k} \parallel [001]$. It has to be mentioned, however, that orthoexciton components of these extreme mass values are not allowed for one-photon quadrupole excitation.[8] They are nevertheless of relevance, since they can be excited by dipole two-photon excitation and they might be of importance in phonon processes.[22]

ACKNOWLEDGMENTS

We acknowledge the support by the Deutsche Forschungsgemeinschaft (SFB Starke Korrelationen im Strahlungsfeld and Grant No. BA1549/18-1).

*dietmar.froehlich@e2.physik.uni-dortmund.de

[1] M. Hayashi and K. Katsuki, J. Phys. Soc. Jpn. **7**, 599 (1952).
[2] E. F. Gross, Usp. Fiz. Nauk. **76**, 433 (1962) [Sov. Phys. Usp. **5**, 195 (1962)]..
[3] S. Nikitine, Prog. Semicond. **6**, 235 (1962).
[4] H. Matsumoto, K. Saito, M. Hasuo, S. Kono, and N. Nagasawa, Solid State Commun. **97**, 125 (1996).
[5] D. Fröhlich, R. Kenklies, C. Uihlein, and C. Schwab, Phys. Rev. Lett. **43**, 1260 (1979); C. Uihlein, D. Fröhlich, and R. Kenklies, Phys. Rev. B **23**, 2731 (1981).
[6] R. J. Elliott, Phys. Rev. **124**, 340 (1961).
[7] G. Dasbach, D. Fröhlich, H. Stolz, R. Klieber, D. Suter, and M. Bayer, Phys. Rev. Lett. **91**, 107401 (2003).
[8] G. Dasbach, D. Fröhlich, R. Klieber, D. Suter, M. Bayer, and H. Stolz, Phys. Rev. B **70**, 045206 (2004).
[9] G. Dasbach, D. Fröhlich, H. Stolz, R. Klieber, D. Suter, and M. Bayer, Phys. Status Solidi C **2**, 886 (2005).
[10] A. Goltztené, C. Schwab, and H. C. Wolf, Solid State Commun. **18**, 1565 (1976).
[11] P. Y. Yu and Y. R. Shen, Phys. Rev. Lett. **32**, 939 (1974); Y. Petroff, P. Y. Yu, and Y. R. Shen, Phys. Rev. B **12**, 1377 (1975).
[12] J. Brandt, D. Fröhlich, C. Sandfort, M. Bayer, H. Stolz, and N. Naka, Phys. Rev. Lett. **99**, 217403 (2007).
[13] G. Baldassarri Höger von Högersthal, G. Dasbach, D. Fröhlich, M. Kulka, H. Stolz, and M. Bayer, J. Luminescence **112**, 25 (2005).
[14] T. Tayagaki, A. Mysyrowicz, and M. Kuwata-Gonokami, J. Phys. Soc. Jpn. **74**, 1423 (2005).
[15] M. French, R. Schwartz, H. Stolz, and R. Redmer, J. Phys. Condens. Matter **21**, 015502 (2009).
[16] G. M. Kavoulakis, Y. C. Chang, and G. Baym, Phys. Rev. B **55**, 7593 (1997).
[17] N. Caswell, J. S. Weiner, and P. Y. Yu, Solid State Commun. **40**, 843 (1981).
[18] D. Fröhlich, J. Brandt, C. Sandfort, M. Bayer, and H. Stolz, Phys. Status Solidi B **243**, 2367 (2006).
[19] D. W. Snoke, D. Braun, and M. Cardona, Phys. Rev. B **44**, 2991 (1991).
[20] M. Jörger, T. Fleck, C. Klingshirn, and R. von Baltz, Phys. Rev. B **71**, 235210 (2005).
[21] K. Yoshioka, T. Ideguchi, and M. Kuwata-Gonokami, Phys. Rev. B **76**, 033204 (2007).
[22] C. Sandfort, J. Brandt, D. Fröhlich, G. Baldassarri Höger von Högersthal, M. Bayer, and H. Stolz, Phys. Rev. B **80**, 245201 (2009).